Supplementary Information

Bioengineering Nisin to overcome the Nisin Resistance Protein

Des Field#[1*], Tony Blake#[3], Harsh Mathur#[2,3], Paula M. O' Connor[2,3], Paul D. Cotter[2,3], R. Paul Ross[1,3] and Colin Hill[1,3]**

[1]School of Microbiology, University College Cork, Cork, Ireland.

[2]Teagasc Food Research Centre, Moorepark, Fermoy, Co. Cork, Ireland.

[3]APC Microbiome Ireland, University College Cork, Ireland.

#DF, TB and HM contributed equally to this work

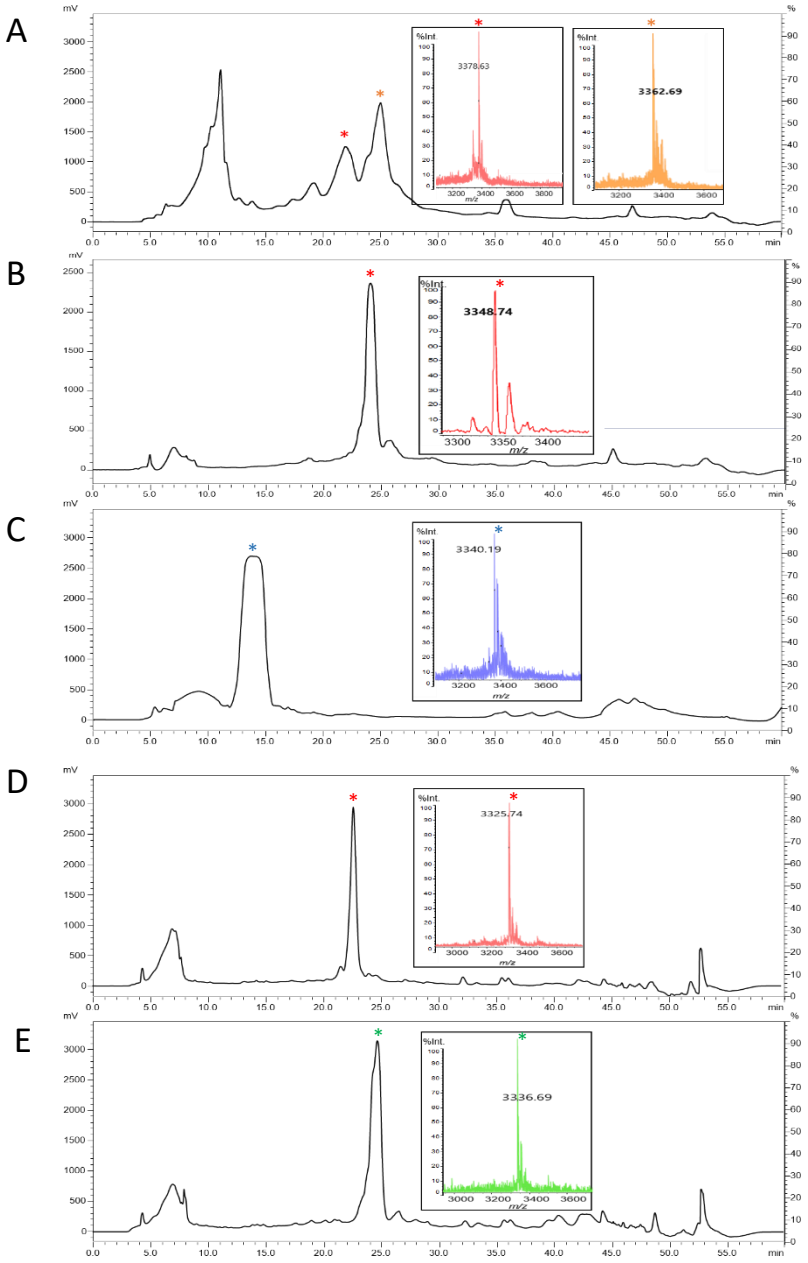

Supplementary Figure 1. RP-HPLC profiles of (A) nisin A S29P and MALDI-ToF mass spectrometric (MS) analysis (inset) of fractions corresponding to nisin A S29P (orange asterisk) and oxidized nisin A S29P (red asterisk), (B) nisin A PV, (C) nisin Z S29P, (D) nisin F S29P and (E) nisin Q S29P developed in a gradient of 30% ACN containing 0.1% TFA to 60 % ACN containing 0.1% TFA from 10 to 40 minutes at a flow rate of 2.2 ml min^{-1}. Purified powder from RP-HPLC fractions were subjected to MS analysis to confirm the expected mass of nisin A S29P (3362 Da), nisin PV (3348 Da), nisin Z S29P (3340 Da), nisin F S29P (3325 Da) and nisin Q S29P (3336 Da).

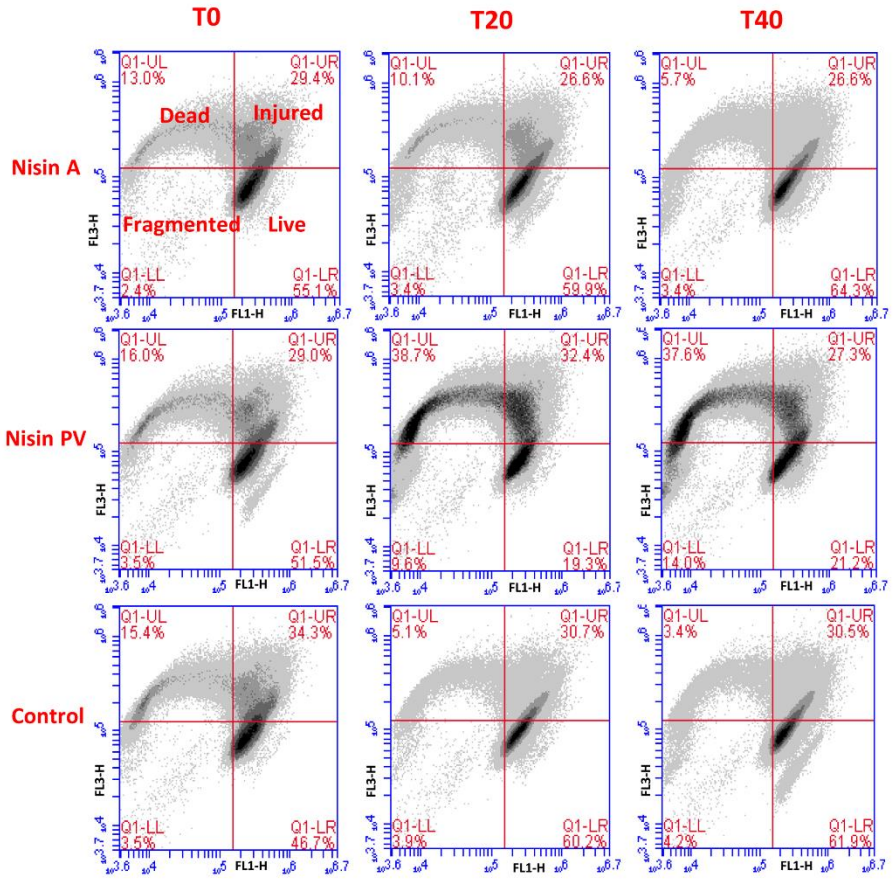

Supplementary Figure 2. Representative plots showing flow cytometry analysis of log-phase *L. lactis* subsp *lactis* biovar *diacetylactis* cells (approximately 1 X 10^7 cfu/ml) exposed to 1 mg/L (0.3µM) nisin A and nisin S29PV peptides and co-stained with Syto9 and PI to assess cell viability and vitality. A cell sample without peptide was prepared as negative control. Populations of live (Syto9) and dead (PI) cells are visible on a PI (FL3-H) vs Syto9 (FL1-H) plot. Samples were analysed upon addition of peptides (T0) and subsequently at 20 mins (T20) and 40 mins (T40).

Supplementary Figure 2 Results:

Similar trends were noted when log-phase cells were treated with 0.3µM nisin A or nisin PV. The number of live cells after 20 minutes was significantly lower when log-phase cells were treated with nisin PV compared to nisin A (P = 0.003587)(Fig. S3 and Figure S4c). Conversely, the number of dead cells was significantly higher for samples treated with nisin PV compared to nisin A (P = 0.003636)(Fig. S3 and S4d). This trend continued after 40 mins of incubation, with a significantly lower number of live cells for samples treated with nisin PV (P = 0.000466) and a significantly higher number of dead cells for samples treated with nisin PV relative to nisin A (P = 0.0014178)(Fig. S3 and S4c). Overall, it can be concluded from the flow cytometry measurements that the live cell population is significantly lower when cells were treated with nisin PV compared to nisin A. Conversely, the numbers of dead cells were significantly higher when samples were treated with nisin PV compared to samples treated with nisin A.

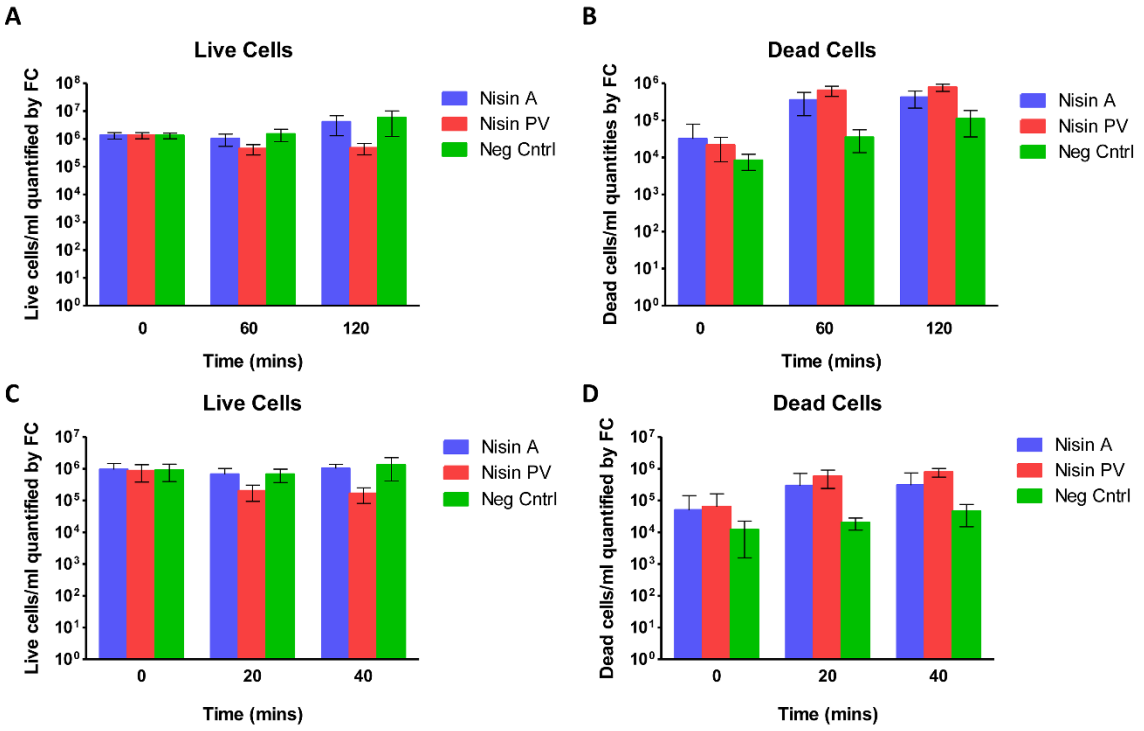

Supplementary Figure 3. Histogram showing live and dead cell population as quantified by flow cytometry: (A) live cells enumerated by flow cytometry for *L. lactis* DRC3 overnight cultures treated with 0.3µM nisin A or nisin PV; (B) dead cells enumerated by flow cytometry for *L. lactis* DRC3 overnight cultures treated with 0.3µM nisin A or nisin PV; (C) live cells enumerated by flow cytometry for *L. lactis* DRC3 log-phase cultures treated with 0.3µM nisin A or nisin PV;(D) dead cells enumerated by flow cytometry for *L. lactis* DRC3 log-phase cultures treated with 0.3µM nisin A or nisin PV.

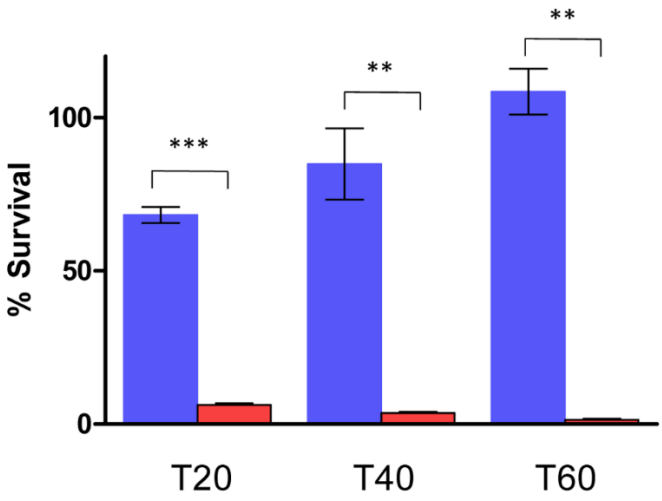

Supplementary Figure 4. Kill curve analysis of *L. lactis* subsp *lactis* biovar *diacetylactis* DRC3 in the presence of nisin A and nisin PV. *L. lactis* subsp *lactis* biovar *diacetylactis* DRC3 exposed to 1.0 mg l^{-1} (0.3 µM) of nisin A (blue) and nisin PV (red) peptides for 20 mins (T20), 40 mins (T40) and 1 hour (T60). Cell survival was measured by performing viable cell counts by dilution of cultures in one-quarter-strength Ringer solution and enumeration on GM17 agar plates. The means and standard deviations of three independent determinations are presented.

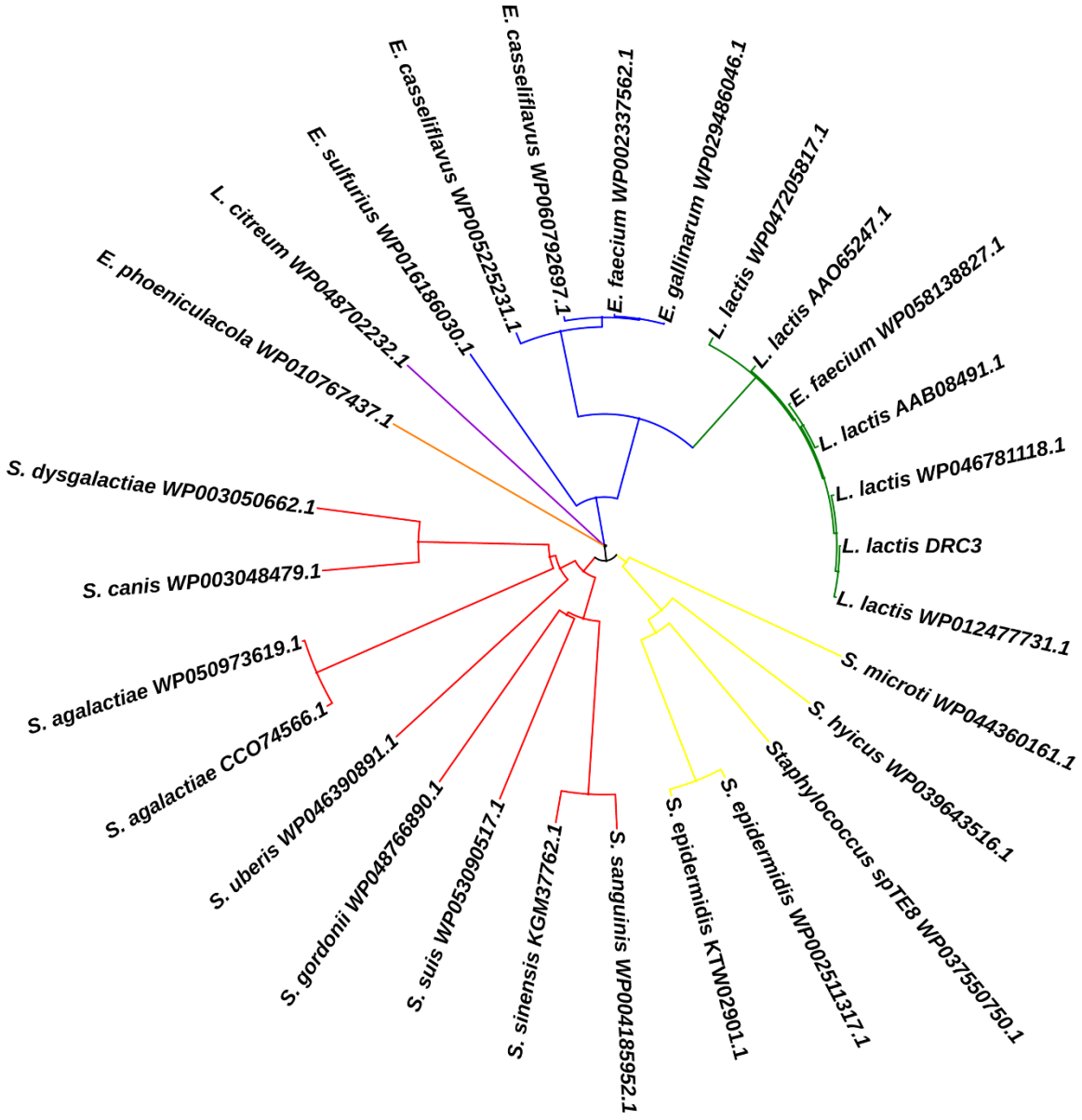

Supplementary Figure 5. A phylogenetic tree of organisms that encode homologues of the nisin resistance protein (NSR). Homologues of NSR were manually retrieved from NCBI following BLASTP (protein-protein blast) search using the NSR sequence from *Lactococcus lactis* subsp *diacetylactis* DRC3 (GenBank Accession No AAA25202.1) as query and visualized using iTOL (Letunic & Bork, 2016).

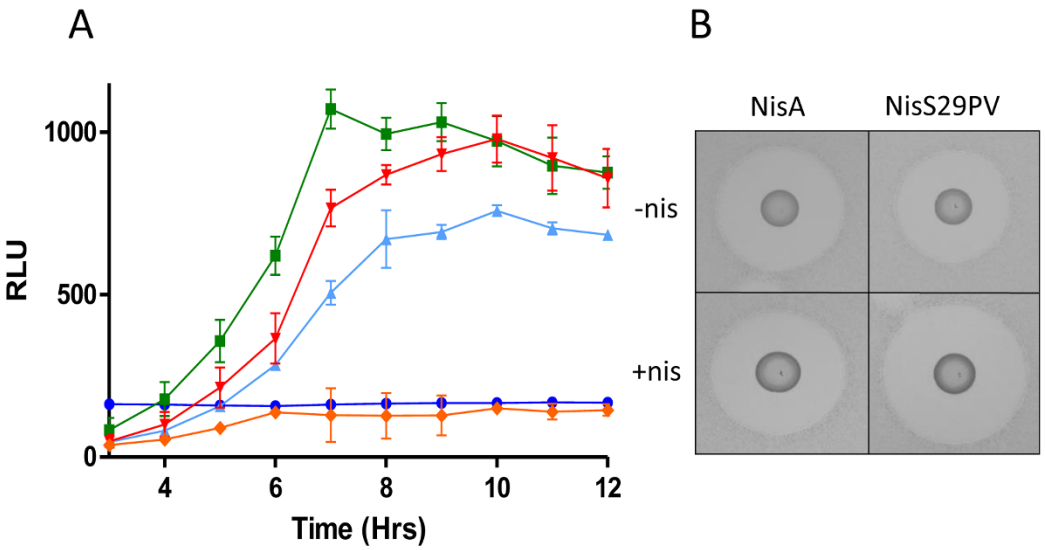

Supplementary Figure 6. (A) Induction capacities (20 ng/ml) of wild type nisin A (green), nisin PV (red), nisin S29P (light blue), truncated nisin A^{1-28} (dark blue) and negative control (orange) as determined by expression of green fluorescent protein (GFP) under control of the nisin promoter and (B) bioactivity of producers of wild type (nisin A) and nisin S29PV in the absence (-nis) or presence (+nis) of nisin.

Supplementary Figure 6 Results: We assessed the induction capacity of the nisin A, nisin A S29P and nisin PV variants given that nisin derivatization can often result in significantly reduced induction ability compared with the wild type peptide (Ge *et al.*, 2016). A sub-inhibitory concentration (20 ng/L) of wild-type nisin A, and the equivalent concentration of nisin A^{1-28} and nisin S29P and nisin PV peptide was added to cells of *L. lactis* NZ9000 pNZ8150*gfp*+, in which *gfp* acts as a reporter of expression from a nisin inducible promoter, and induction of GFP was monitored over 12 hours in terms of relative fluorescence units (RFU) (Fig. 6A). As expected, the truncated nisin A^{1-28} peptide failed to produce any fluorescence signal, in agreement with previous studies that established the need for about 400- or 500-fold higher concentration of $nisin^{1-28}$ to induce the same GFP intensity as nisin A (Liang *et al.*, 2010). NZ9000 pNZ8150*gfp*+ cells in the presence of nisin S29P and nisin PV produced a lower fluorescence signal overall, in addition to a slower rate of induction (Supplementary Fig 6A), relative to those exposed to nisin A. Furthermore, when the *L. lactis* nisin PV producing strain was subjected to induction with nisin A added to the growth medium (GM17 agar), a significantly larger zone of inhibition was observed than that of its counterpart in the absence of inducer peptide (Supplementary Fig. 6B).

Supplementary Table 1. Strains and plasmids utilised in this study.

Strains	**Relevant characteristics**	**Reference**
L. lactis NZ9700	Wild type nisin producer	(Kuipers *et al.*, 1998, Kuipers *et al.*, 1993)
L. lactis NZ9800	*L. lactis* NZ9700Δ*nis*A	(Kuipers *et al.*, 1998, Kuipers *et al.*, 1993)
L. lactis NZ9800pDF05	*L. lactis* NZ9800 harboring pCI372 with nisA under its own promoter	(Field *et al.*, 2008)
L. lactis NZ9800pDF22	*L. lactis* NZ9800 harboring pCI372-nisA$^{1\text{-}28}$	This study
L. lactis NZ9800 pCI372-nisQ	*L. lactis* NZ9800 harboring pCI372-nisQ	(Piper *et al.*, 2011)
L. lactis NZ9000	Most commonly used host of the NICE system.	(Kuipers *et al.*, 1998, Kuipers *et al.*, 1993)
L. lactis NZ9000pNZ8150	*L. lactis* NZ9000 harboring pNZ8150, *Sca*I site used for translational fusions, standard NICE vector; Cm^{R}	(Mierau & Kleerebezem, 2005)
L. lactis NZ9000pDF18	*L. lactis* NZ9000 harboring pNZ8150-gfp+ under the nisin promoter	This Study
E. coli Top10	Intermediate cloning host	Invitrogen
Indicator organisms		
L. lactis subsp. *diacetylactis* DRC3	*L. lactis* strain that carries the nisin-resistance gene *nsr on the plasmid pNP40*	(Froseth & McKay, 1991)
L. lactis spp *cremoris* HP	Nisin sensitive indicator	UCC Culture Collection
L. lactis MG1614	Nisin sensitive indicator. Rifampicin- and streptomycin-resistant derivative of MG1363	(Gasson, 1983)
L. lactis MG1614pNP40	*L. lactis* strain that carries the nisin-resistance gene *nsr on the plasmid pNP40*	(O'Driscoll *et al.*, 2006)
S. uberis ATCC 700407	Quality control strain for API products (API 78-11-025)	ATCC reference strain
S. uberis DPC5344	Mastitis-associated indicator organism	DPC Culture Collection
E. casseliflavus DPC5053	Nisin sensitive indicator (VanC phenotype).	DPC Culture Collection

Supplementary Table 2. Oligonucleotides utilised in this study.

Primer name	Sequence
NisAS29XXdeg For	5'- PHO TGT CAT TGT NNK NNK CAC GTA AGC AAA TAA TCT AGA-3'
NisAS29XXdeg Rev	5'- GCT TAC GTG MNN MNN ACA TAG ACA AGT TGC TGT TTT CAT GTT-3'
NisZS29deg FOR	5' Pho- GCA ACT TGT AAC TGT NNK ATT CAC GTA AGC AAA TAA TCT AGA
NisZS29deg REV	5' GCT TAC GTG AAT MNN ACA GTT ACA AGT TGC TGT TTT CAT GTT
NisFS29deg FOR	5' Pho- GCA ACT TGT AAC TGT NNK GTT CAC GTA AGC AAA TAA TCT AGA
NisFS29deg REV	5' GCT TAC GTG AAC MNN ACA GTT ACA AGT TGC TGT TTT CAT GTT
NisQS29deg FOR	5' Pho- GCA ACT TGT AAC TGT NNK GTT CAC GTA AGC AAA TAA TCT AGA 3'
NisQS29deg REV	5' GCT TAC GTG AAC MNN ACA GTT ACA AGT TGC TGT TTT CAG 3'
NisA1-28For	5'-TGTCATTGTTAAATTCACGTAAGCAAATAATCTAGA-3'
NisA1-28Rev	5'-TACGTGAATTTAACAATGACAAGTTGCTGTTTTCATGTT-3'
oDF107	5' GCTCTAGATTATTTGTAGAGCTCATC-3'
oDF109	5'-CCGGGATATCATGAGTAAAGGAGAAGAA-3'
pNZ44For	5′ TTACAGGTACATCATTCTGTTTGT 3′
pNZ44 Rev	5′ TGTTTTAACGATTATGCCGATAAC 3′
pCI372For	5'- CGGGAAGCTAGAGTAAGTAG -3'
pCI372Rev	5'- ACCTCTCGGTTATGAGTTAG -3'

Supplementary Table 3. Mass Spectrometry results of producing strains from the S29X banks in the nisin Z, nisin F and nisin Q backgrounds.

Amino acid	NisinZ-S29X	NisinF-S29X	NisinQ-S29X
N	3358.92	3341.45	nd
Q	3372.41	nd	3367.38
C	nd	nd	nd
G	3300.64	3286.77	3299.07
A	3314.55	3299.41	3311.85
S	3331.63(WT)	3316.85(WT)	3327.50(WT)
T	3344.91	3329.03	3342.64
V	3343.08	3327.44	3340.10
L	3356.42	3341.95	3353.85
I	3356.06	3340.50	3353.85
P	3341.27	3326.56	3338.64
M	3374.82	3360.86	nd
F	3390.79	3376.40	nd
Y	3407.16	3394.39	3403.74
W	3429.48	3415.04	nd
D	3355.30	3343.60	3354.11
E	3373.15	3357.93	3367.97
R	3399.69	3385.13	3397.29
H	nd	3364.28	3376.93
K	3372.66	nd	nd

Supplementary Methods

Kill curve assays

For peptide kill assays, fresh overnight cultures of *Lactococcus lactis* subsp. *lactis* biovar *diacetylactis* DRC3 were transferred (10^7 cfu ml^{-1} in a volume of 1.0 ml.) into GM17 broth containing the relevant concentration of wild-type or mutant nisin and incubated for 60 mins at 37°C. Cell viability was measured by performing viable cell counts at 20, 40 and 60 mins by diluting cultures in one-quarter-strength Ringer solution and enumeration on GM17 agar plates.

Construction of a nisin-inducible GFP expression plasmid

The pNZ8150 plasmid expressing the reporter protein GFP was created as follows. The *gfp*$^+$ gene was amplified from plasmid pEVS*gfp*+ (Lango-Scholey *et al.*, 2013) by using primers *oDF107* and *oDF109* (Table S1) containing the Xba1 and EcoRV restriction sites. The cloning vector pNZ8150 (contains a *Sca*I site used for translational fusions to the inducible promoter

P_{nisA}) (Mierau & Kleerebezem, 2005) was digested with Sca1 and Xba1 restriction enzymes while the amplified *gfp* insert were digested with EcoRV and Xba1 and subsequently ligated together. The resulting pNZ8150*gfp+* plasmid was transformed into chemically competent *E. coli* Top cells (Invitrogen). Plasmid DNA was extracted and the *gfp+* insert was amplified using pNZ44For and pNZ44Rev (Table S1), sequenced (Source BioScience, Waterford, Ireland) to ensure integrity and subsequently transformed into *L. lactis* NZ9000 host cells.

Structural model of nisin and nisin PV bound to NSR

The molecular modelling simulations consisted of 2 models. The first model used a configuration of residues 22-34 of a nisin mutant where residue 29 is serine and is structurally aligned so that residues 22-34 fit into the tunnel region of the NSR molecule. The second model was also aligned to fit into the tunnel region of the NSR enzyme only this time residue 29 has been mutated to proline and residue 30 had been mutated to valine. To create a pdb file for the NSR-nisin complex individual pdb files for both NSR and nisin were required. This was carried out with relative ease using the R package bio3d(Grant *et al.*, 2006). For the NSR molecule the pdb file *4Y68* was used and for the nisin the *1wco* pdb file was used where Protein Databank Accession number for both files came from their respective papers (Khosa *et al.*, 2016, Hsu *et al.*, 2004)To determine a starting configuration for the NSR-nisin complex a docking program Autodock for ligand and protein binding was used(Morris *et al.*, 2009). In the Using AutoDock 4 and AutoDock Vina with AutoDockTools:A Tutorial exercises 1-10 were followed to carry out the docking procedure with *1wco.pdb* as the ligand and *4Y68.pdb* as the receptor. This produced 9 possible binding conformations for the NSR-nisin complex. Out of these 9 states the 7th conformation state was chosen being the state which showed most favorable interaction between residues 29 of nisin and residues 236-240 of the active site in NSR. In this model the NSR-nisin complex had serine for residue 29. The molecular visualisation package CHIMERA(Pettersen *et al.*, 2004) was then used to mutate residue 29 to proline(Dunbrack, 2002) and the subsequent configuration saved as a different pdb file. Again the docking program Autodock was used to create a starting configuration for the NSR-nisin complex. In this case the 1st conformation was chosen for the same reasons as previously. Then both chosen conformation states (one with serine, the other with proline) were saved as separate pdb files to be used as starting configurations in the molecular modeling simulation. In what follows the procedure for workflow as applied to the NSR-nisin model with serine is described. The steps for the workflow as applied to the NSR-nisin model with proline are identical. Here the *Amber 16* suite of programs was used(Case *et al.*, 2016). To start, the pdb files from the docking procedure step were prepared for use with Amber's LEaP program. The *pdb4amber* program changed the residues labled HIS to HIE and indicated that the nonstandard residues dehydroalanine (DHA) and d-alpha-aminobutyric acid (DBB) were not recognised by LEaP. Also the *reduce* program with the -Trim flag strips all hydrogens from the pdb file(Word *et al.*, 1999). To deal with the nonstandard residues dehydroalanine (DHA) and d-alpha-aminobutyric acid (DBB) the respective entries in the RCSB Protein Data Bank were accessed and the respective *.cif* files downloaded. The amber program *antechamber* can read the *.cif* files of the nonstandard residues and assign partial charges and atom types to the nonstandard residues based on the *bcc charge scheme*(Jakalian *et al.*, 2002). This will output *.ac* files which have charge and bonding information for the nonstandard residues. These will then be used as input to the *prepgen* program along with a custom made *.mc* file that tells the *prepgen* program what

atoms to ignore from the residue (for peptide bonding). The prepgen program then outputs *.prepin* files which are then inputed into the *parmchk2* program that creates the *.frcmod* files using parameters from the *gaff.dat* and *parm10.dat* parameter files. Next the *.prepin* and *.frcmod* files were read into the LEaP program. Values from the *gaff2.dat* file were used as the values for the missing parameter indicated by LEaP. The underlying cause of the "missing parameter" issue was LEaP's inability to recognise the 3 peptide bonds and associated angles and dihedral angles of LYS-DBB, ALA-DBB, and VAL-DHA. Thus the *extra.frcmod* file was created to supply these missing values to LeaP. All other parameters were taken from the ff14SB force field. LEaP was then used to build back up all stripped hydrogens, solvate the system using the TIP3 water model and neutralise using counter ions. Next the *sander* program was used to carry out the molecular simulation. To use this program an input file needed to be created that would inform the program of the physical processes to simulate. Noting the good results of a previous study(Khosa *et al.*, 2016), the same parameters were employed. Firstly the system was minimised in a two stage process. This means that harmonic restraints with a force constant of 25 $kcal.mol^{-1}Å^{-2}$ were applied to all protein atoms while all other atoms were free to move during 50 cycles of steepest descent (SD) and 200 cycles of conjugate gradient (CG) minimization. In the second stage (using a separate input file with adjusted parameters, min2.in), the force constant of the harmonic restraints was reduced to 5 $kcal.mol^{-1}Å^{-2}$, and 50 cycles of SD and 200 cycles of CG minimization were performed. The sander program takes the input file *min.in* with the instructions on how to minimise, the topology file *com.wat.neutral2.prmtop* also as input, the coordinate file *com.wat.neutral2.prmcrd* again as input and the coordinate file to act as reference for the restraint intsructions. It outputs the *min.out* file that contains information on each time step of the minimisation phase and a restart file *01_Min.rst* so the command for the second stage knows the coordinates of where to start from. Next the system is heated up for a period of 50 picoseconds from 100K ro 300K with volume held constant. This is the input file for the heating stage. Then the density was adjusted to 1 $g \cdot cm^{-3}$ during 30 ps while keeping pressure constant. Next the positional restraints were gradually reduced from 5 $kcal.mol^{-1}Å^{-2}$ to 0 $kcal.mol^{-1}Å^{-2}$ while keeping the volume constant. This was achieved in the MD simulation by a series of 6 stages (each stage having a different input file with the value for *restraint_wt* going from 5 to 0). Each stage was 10 picoseconds long. All of these processes create the trajectory files which have the extension *.mdcrd* . These are the most important files (trajectory files) as they contain the binary information that the programs *cpptraj* and *MMPBSA.py* will make use of to analyse the MD trajectories. Finally the input file was changed to instruct a production run of 50 nanoseconds. This meant setting the total number of timesteps to 25000000. The command to run this part of the simulation uses the parallel processes program MPI (as otherwise it would take several years to complete the simulation). Throughout the full MD simulation long-range electrostatic interactions were treated using the particle mesh Ewald method(Darden *et al.*, 1993, York *et al.*, 1993)A distance cut off of 8 Å was used to define short range electrostatic interactions. All bonds involving hydrogen were constrained by using the SHAKE algorithim(Ryckaert *et al.*, 1977) which also required setting the timestep to be 2 femtoseconds. Trajectory files were created every picosecond. To analyse the MD trajectory the programs *cpptraj* and *MMPBSA.py* were used. To calculate the distance between the carbonyl carbon of CYS28 (NSR cleave point in nisin) and the sidechain Oxygen in residue 236 of NSR (active site) the *dist* command in *cpptraj* was used. The only requirements for *cpptraj* were the topology file *com.wat.neutral2.prmtop* and an input file specifying what trajectory files were to be used. After the trajectory analysis has finished the output file SER236OtoCYS28C contains the distance between both points of interest for every picosecond of the trajectory. These can then be plotted using the *ggplot2* program in R. The next part of the trajectory analysis involves determining what hydrogen bonds have formed over the duration of the simulation (35 nanoseconds). This was achieved

by again using the *cpptraj* program and a different input file. The important file to note is the *All.UU.avg.dat* file. This contains all the percentages for hydrogen bond formation over the course of the trajectory. After the hydrogen bond calculation the *MMPBSA.py* was used to calculate the binding energies of the residues in nisin and the residues in the active site of (TASSAEM motif) NSR. This also required many of the files prepared earlier in the analysis using the LEaP program. One final point to note. For the binding energy calculations the MM-GBSA (Generalised Born) method was used and not the MM-PBSA (Poisson-Boltzmann) method. The *FINAL_DECOMP_MMPBSA.dat* file has all the values of the binding energies for the residues specified in the input file and can then plotted using the *ggplot2* package in R.

Induced expression of *gfp+* by native nisin A, nisin A PV and truncated Nisin$^{1-28}$

For induction experiments, overnight cultures of *L. lactis* NZ9000 pNZ8150*gfp+* were diluted 1:100 and added to fresh medium (GM17) and incubated at 30 °C until the absorbance of the medium at 600 nm (A_{600}) reached 0.5. Next, wild-type nisin A, nisin A$^{1-28}$ and nisin PV peptides were added to a final concentration of 20 ng/L. Subsequently 1.5 mls was transferred to 24 well microtitre plates (4titude Surrey, UK). Green protein fluorescence was detected in terms of relative fluorescence units (RFU) with a SpectraMax M3 spectrophotometer (Molecular Devices, Sunnyvale, Calif.) with excitation and emissions filters set to 485 and 538 nm. The baseline fluorescence of the growth medium prior to inoculation was subtracted from all subsequent fluorescence readings using SoftMax Pro v6.3 software).

Statistical analysis

Flow cytometry data was analysed using a 1-tailed t-test in Microsoft Excel 2010 to determine statistically significant differences between sub-populations for samples treated with nisin PV compared to samples treated with nisin A.

Kill curve statistical analysis was carried out using an unpaired Students t-test in GraphPad Prism software following analysis by SPSS to show data was normally distributed.

Supplementary References

Case, D.A., R.M. Betz, D.S. Cerutti, T.E.I. Cheatham, T.A. T.Darden, R.E. Duke, T.J. Giese, H. Gohlke, A.W. Goetz, N. Homeyer, S. Izadi, P. Janowski, J. Kaus, A. Kovalenko, T.S. Lee, S. LeGrand, P. Li, C. Lin, T. Luchko, R. Luo, B. Madej, D. Mermelstein, K.M. Merz, G. Monard, H. Nguyen, H.T. Nguyen, I. Omelyan, A. Onufriev, D.R. Roe, A. Roitberg, C. Sagui, C.L. Simmerling, W.M. Botello-Smith, J. Swails, R.C. Walker, J. Wang, R.M. Wolf, X. Wu, l. Xiao & P.A. Kollman, (2016) AMBER 2016, . *University of California, San Francisco.*

Darden, T., D. York & L. Pedersen, (1993) Particle mesh Ewald: An N·log(N) method for Ewald sums in large systems. *The Journal of Chemical Physics* **98**: 10089-10092.

Dunbrack, R.L., Jr., (2002) Rotamer libraries in the 21st century. *Current opinion in structural biology* **12**: 431-440.

Field, D., P.M.O. Connor, P.D. Cotter, C. Hill & R.P. Ross, (2008) The generation of nisin variants with enhanced activity against specific Gram-positive pathogens. *Molecular Microbiology* **69**: 218-230.

Froseth, B.R. & L.L. McKay, (1991) Molecular characterization of the nisin resistance region of Lactococcus lactis subsp. lactis biovar diacetylactis DRC3. *Applied and Environmental Microbiology* **57**: 804-811.

Gasson, M.J., (1983) Plasmid complements of *Streptococcus lactis* NCDO 712 and other lactic streptococci after protoplast-induced curing. *J Bacteriol* **154**: 1-9.

Ge, X., K. Teng, J. Wang, F. Zhao, F. Wang, J. Zhang & J. Zhong, (2016) Ligand determinants of nisin for its induction activity. *Journal of Dairy Science* **99**: 5022-5031.

Grant, B.J., A.P.C. Rodrigues, K.M. ElSawy, J.A. McCammon & L.S.D. Caves, (2006) Bio3d: an R package for the comparative analysis of protein structures. *Bioinformatics* **22**: 2695-2696.

Hsu, S.T., E. Breukink, E. Tischenko, M.A. Lutters, B. de Kruijff, R. Kaptein, A.M. Bonvin & N.A. van Nuland, (2004) The nisin-lipid II complex reveals a pyrophosphate cage that provides a blueprint for novel antibiotics. *Nature structural & molecular biology* **11**: 963-967.

Jakalian, A., D.B. Jack & C.I. Bayly, (2002) Fast, efficient generation of high-quality atomic charges. AM1-BCC model: II. Parameterization and validation. *J Comput Chem* **23**: 1623-1641.

Khosa, S., B. Frieg, D. Mulnaes, D. Kleinschrodt, A. Hoeppner, H. Gohlke & S.H. Smits, (2016) Structural basis of lantibiotic recognition by the nisin resistance protein from *Streptococcus agalactiae*. *Scientific reports* **6**: 18679.

Kuipers, O.P., M.M. Beerthuyzen, R.J. Siezen & W.M. De Vos, (1993) Characterization of the nisin gene cluster nisABTCIPR of *Lactococcus lactis*. Requirement of expression of the nisA and nisI genes for development of immunity. *European journal of biochemistry* **216**: 281-291.

Kuipers, O.P., P.G. De Ruyter, M. Kleerebezem & W.M. De Vos, (1998) Quorum sensing-controlled gene expression in lactic acid bacteria. *J Biotechnol* **64**: 15-21.

Lango-Scholey, L., A.O. Brachmann, H.B. Bode & D.J. Clarke, (2013) The expression of *stl*A in *Photorhabdus luminescens* is controlled by nutrient limitation. *PloS one* **8**: e82152.

Letunic, I. & P. Bork, (2016) Interactive tree of life (iTOL) v3: an online tool for the display and annotation of phylogenetic and other trees. *Nucleic acids research* **44**: W242-245.

Liang, X., Z. Sun, J. Zhong, Q. Zhang & L. Huan, (2010) Adverse effect of nisin resistance protein on nisin-induced expression system in *Lactococcus lactis*. *Microbiological Research* **165**: 458-465.

Mierau, I. & M. Kleerebezem, (2005) 10 years of the nisin-controlled gene expression system (NICE) in Lactococcus lactis. *Applied microbiology and biotechnology* **68**: 705-717.

Morris, G.M., R. Huey, W. Lindstrom, M.F. Sanner, R.K. Belew, D.S. Goodsell & A.J. Olson, (2009) AutoDock4 and AutoDockTools4: Automated Docking with Selective Receptor Flexibility. *Journal of computational chemistry* **30**: 2785-2791.

O'Driscoll, J., F. Glynn, G.F. Fitzgerald & D.v. Sinderen, (2006) Sequence analysis of the lactococcal plasmid pNP40: a mobile replicon for coping with environmental hazards. *Journal of Bacteriology* **188**: 6629-6639.

Pettersen, E.F., T.D. Goddard, C.C. Huang, G.S. Couch, D.M. Greenblatt, E.C. Meng & T.E. Ferrin, (2004) UCSF Chimera--a visualization system for exploratory research and analysis. *J Comput Chem* **25**: 1605-1612.

Piper, C., C. Hill, P.D. Cotter & R.P. Ross, (2011) Bioengineering of a nisin A-producing *Lactococcus lactis* to create isogenic strains producing the natural variants nisin F, Q and Z. *Microbial Biotechnology* **4**: 375-382.

Ryckaert, J.-P., G. Ciccotti & H.J.C. Berendsen, (1977) Numerical integration of the cartesian equations of motion of a system with constraints: molecular dynamics of n-alkanes. *Journal of Computational Physics* **23**: 327-341.

Word, J.M., S.C. Lovell, T.H. LaBean, H.C. Taylor, M.E. Zalis, B.K. Presley, J.S. Richardson & D.C. Richardson, (1999) Visualizing and quantifying molecular goodness-of-fit: small-probe contact dots with explicit hydrogen atoms. *Journal of molecular biology* **285**: 1711-1733.

York, D.M., T.A. Darden & L.G. Pedersen, (1993) The effect of long-range electrostatic interactions in simulations of macromolecular crystals: A comparison of the Ewald and truncated list methods. *The Journal of Chemical Physics* **99**: 8345-8348.